

# Ultrasonic rangefinder with the submillimeter resolution as a part of the rescue robot's sensor system

S Goll<sup>1,2</sup> and J Maximova<sup>1,2</sup>

<sup>1</sup>Department of Information-Measuring and Biomedical Engineering, Ryazan State Radio Engineering University (RSREU), Gagarin Street, 59/1, Ryazan, RU

<sup>2</sup>LLC KB Avrora, Skomoroshinskaja Street 9, of.3, Ryazan, RU

**Abstract.** The main goal of the research is to increase the measurement resolution of the ultrasonic rangefinders to meet the needs of vital signs noncontact registration based on the chest movements. The two-phase method is proposed to make distance estimates by sending the probe pulse trains, calculating the phase spectrum of the echo signal's envelope and tracking its relevant components. During the first phase the rough TOF based estimate is made. During the second phase this estimate is corrected based on the phase spectrum of the echo signal's envelope, the phase ambiguity is removed and the relevant components are determined. The final estimate of the human chest displacement is calculated based on these relevant components. The output data rate is the same as for the TOF measurements, but the measurement resolution is increased to the one hundredth of the ultrasonic wavelength. The experiment results are provided for the both model and the real human chest displacements caused by the respiration and heartbeat processes.

## 1. Introduction

The extreme mobile robotic systems, the safety-critical systems (particularly, the ones designed for the drivers, pilots, motormen) as well as medical equipment (e.g., diagnostic and therapy instruments) need the low-cost precision rangefinders with the effective range up to 1 meter and the output data rate of at least 20 Hz to measure both absolute and relative distances. Such rangefinder sensors can be used to provide the noncontact measurements of the person's pulse and respiratory rates – the information critical for the rescue operations planning, human-factor accidents prevention and the medical equipment synchronization with the patient's biorhythms [1].

Search and Rescue (SAR) operations caused by industrial disasters and military conflicts can be dangerous for the SAR crew members. The main tendency here is to minimize the human presence in the dangerous zone by relying on the telemetry data (i.e., victims' vital signs and locations) to optimally plan and execute the rescue operation, including the SAR crew members' efforts and the rescue robots, both autonomous and remote controlled.

Detection of the injured person's vital signs, mainly pulse and respiratory rates, poses a nontrivial task even for a remote controlled rescue robot. For that task video and thermal cameras are considered to be the most informative sensors. Due to amount of data broadcasted by these sensors, they require wired connection (e.g., LAN) between the robot and the human operator or the broadband wireless connection in case the former is not possible. However, the radio wave-based data transmission can lead to detection mistakes due to interferences and non-line-of-sight and near-line-of-sight transmissions. Moreover, the usage of thermal camera to detect the body temperature can sometimes lead to the dead body being mistaken for the living person.

Another way to measure the human vitals is to make contact measurements. In that case robot must place the electrodes on the particular parts of the human body, which leads to a handful of problems like the process of electrodes placement or detection and recognition of the body parts where the electrodes should be placed. Clearly, these can be quite dangerous operations to be performed on an injured person.

## 2. Related work

The noncontact measurements of the pulse and respiratory rates can be taken by the means of the short-range radars since it is possible for the single integrated circuit to contain two 77 GHz UHF transmission lines (one transmitting line and one receiving line) as well as the low-frequency processing channel and the ADC [2]. The data gathered that way can be affected by the electromagnetic interference and other factors; hence, we propose to increase the robustness of the radar measurements by the means of the secondary noncontact measurement channel based on the ultrasonic sensors.

The commonly used Time-of-Flight Principle [3] is based on the measurement of the time interval between the start of the ultrasonic wave emission and the moment when the reflected wave causes the difference between the current air pressure and the air pressure at rest to exceed the given threshold for the first time. The measurement resolution of the ToF-based sensor depends both on the properties of the Timer/Counter used and the ultrasonic signal wavelength. The ToF measurement resolution for the 40 kHz ultrasound is, at a rough estimate, of 8 mm. At the same time, a lot of the ToF-based sensors are featured with the resolution up to the one fourth of the ultrasonic wavelength. To achieve such resolution various methods can be used: the adaptive threshold, comparisons for the positive and negative half-waves, etc. However, all these modifications are not enough to achieve the submillimeter resolution.

Another attempts to improve the measurement resolution of the ultrasonic rangefinders are based on the Linear Frequency Modulation or Composite Modulation [4]. However, these methods require broadband ultrasonic receivers and transmitters sufficiently increasing the hardware cost.

## 3. The approach

In this paper we propose an algorithm to improve the measurement resolution of the low-cost single-tone 40 kHz ultrasonic rangefinders. These inverse piezoeffect based sensors are commonly used in the automotive industry to build Advanced Driver Assistance Systems (ADAS).

The cyclic movements of the human chest are caused by both the respiration process and the cardiac activity with the movement amplitudes of 4 to 12 mm and 0.5 mm accordingly [5]. The cardiac cycle is more frequent than the respiration cycle and able to occur up to 200 times per minute. According to the Nyquist–Shannon–Kotelnikov sampling theorem the measurement rate of 20 Hz is sufficient to perform the vital signs detection. Due to the comparatively high sound speed in the air medium it is possible to obtain up to 100 measurements per second at the distance of up to 1 meter using the ToF method. Despite this, the measurement resolution of one fourth of the 40 kHz ultrasonic wavelength is deficient in pulse and respiratory rates registration.

We suggest an approach to improve the measurement resolution without changing the output data rate. First, some (for example, ToF) method is used to obtain a rough distance estimate  $d_{ref}$ . Second, the proposed method is used to  $d$  estimate the displacement relative to the rough estimate  $d_{ref}$ . Opposing to the ToF method which uses the point in time when the threshold is exceeded as the input data, the proposed method uses all the readings of the echo signal gathered with the sampling rate  $f_d = 200 \text{ kHz}$ .

The figure 1a shows pulse trains containing  $N = 8$  probe pulses each with the probe pulse frequency set to  $f_{us} = 40 \text{ kHz}$ . The pulse trains are transferred to ultrasonic transmitter with the frame period  $T = 10 \text{ ms}$ . The black-colored regions in the figure 1b represent the digital signal  $u$  which is formed from the received frame sequence and can be described as the amplitude overmodulated

signal. The white line in the figure 1b represents the demodulated envelope of the receiver's signal. To compute the envelope the modulated signal is multiplied by the sinusoidal carrier signal  $v = V\sin(2\pi f_{us}t + \varphi_v)$  sampled with the rate  $f_d$ ; then the low pass recursive filter with the transfer function  $\frac{b_0z^2+b_1z+b_2}{z^2+a_1z+a_2}$  is applied to the multiplication result. The figure 1c shows the enlarged version of the frame surrounded with the dotted rectangle in the figure 1b. Each frame contains the deterministic transmitted pulse received when the transmitter emits the ultrasonic wave. This signal starts from the beginning of the frame and ends at time  $t_1$ . In the case some object or group of objects is present in the area covered by the rangefinder's beam pattern and these objects are large enough to reflect the ultrasonic wave with the frequency  $f_{us}$ , the frames also contain the reflected echo signal at the time interval  $\Delta t = [t_2 \dots t_3]$ .

The moment  $t_1$  when the transmitted pulse ends is constant for every frame and is computed as  $t_1 = \frac{N + n_1}{f_{us}}$ . We define the frame containing the rough ToF-based measurement of the distance  $d_{ref}$  to the closest object in the sensor's beam pattern as a reference frame. The rough estimate  $d_{ref}$  is proportional to the time interval  $t_{ref}$  which is determined when the echo signal exceeds the comparison threshold  $u_{ref}$  after the time  $t_1$ . For the every frame received after the reference frame time  $t_2 = t_{ref} - \frac{n_2}{f_{us}}$  remains constant until the new reference frames arrives changing the value of  $t_{ref}$ . The coefficients  $n_1$  and  $n_2$  represent the adjustable offsets with the integer values.

The reference frame is used as a starting point for the proposed method to compute its distance estimate and can be set (and changed later) either by the human operator's request or automatically if the absolute distance measurements acquired by the means of the ToF method lie in some predetermined intervals. The moment  $t_3 = t_2 + \Delta t$  sets the right boundary of the echo signal's time interval of the constant duration  $\Delta t = const$ .

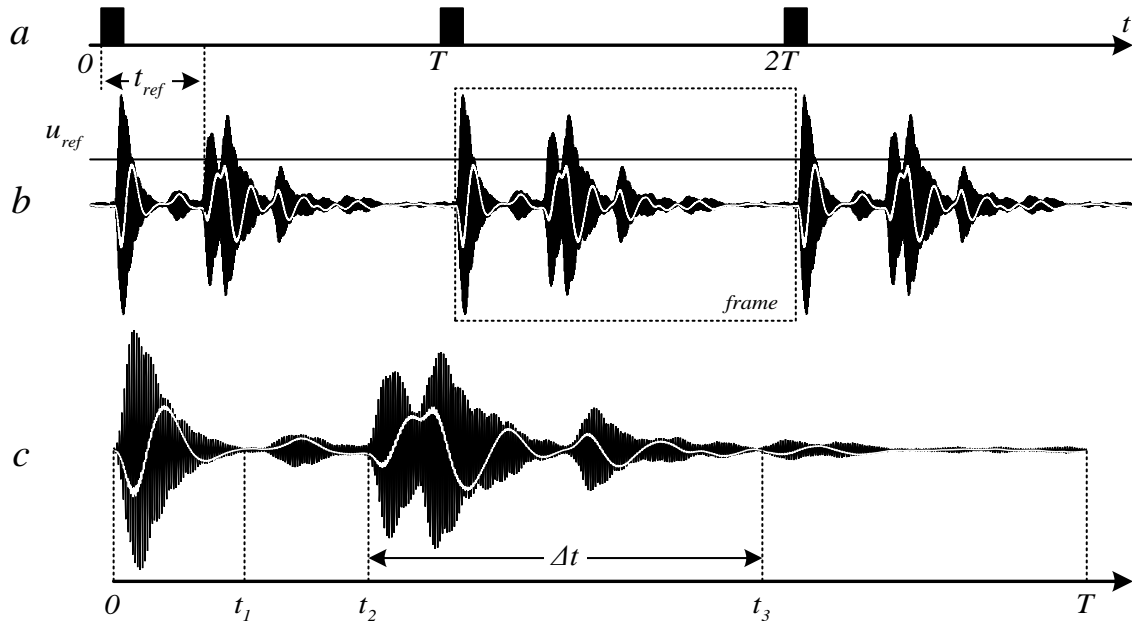


**Figure 1.** a – probe pulse trains, b – received reflected signal, c – a single frame as it appears in the receiver.

On the  $\Delta t = [t_2 \dots t_3]$  interval of the each frame the Fast Fourier Transform is applied to the echo signal's envelope and then for the each of its frames the phase spectrum is computed.

The next step is the selection of the  $M = 10$  sequential spectrum components starting with the 2<sup>nd</sup> component which are expressed as  $\vec{\varphi}[k] = (\varphi_1[k] \ \varphi_2[k] \ \dots \ \varphi_M[k])^T$ , where  $k$  is the number of frame relative to the reference frame. This selection takes place at the end of the each frame period  $T$ . Each component  $\varphi_m[k]$  is used to estimate the displacement  $d_m[k]$  relative to the rough estimate  $d_{ref}$ . This estimate is calculated as  $d_m[k] = \varphi_m[k] + \lambda_m[k] \cdot \pi$ , where  $\lambda_m[k]$  is the number of  $m^{\text{th}}$  component's phase unwrappings and is calculated as follows:

$$\lambda_m[k] = \lambda_m[k-1] + g(\Delta\varphi_m[k]), \quad (1)$$

where  $\Delta\varphi_m[k] = \varphi_m[k] - \varphi_m[k-1]$ ,  $g(\zeta) = \begin{cases} -1, & \zeta < -\varphi_{ref} \\ 1, & \zeta > \varphi_{ref} \\ 0, & \text{otherwise} \end{cases}$ ,  $\varphi_{ref}$  is the adjustable threshold of the

$\Delta\varphi_m[k]$ .

The figure 2 illustrates the computation of the displacement  $d_m[k]$ . When the new reference frame is set the number of phase unwrappings  $\lambda_m[0]$  is zeroed for the each phase component which provides the recurrent expression (1) with the initial condition. Therefore, for the each received frame the  $M = 10$  estimates are calculated for the absolute distance  $h_m$  between the sensor and the object of interest. Each of these estimates is calculated as  $h_m[k] = d_{ref} + d_m[k]$ , where  $m = 1, 2, \dots, M$ , and, apparently, represents the sum of the reference distance  $d_{ref}$  and the displacement  $d_m[k]$  computed using the proposed method. Let us note that  $N$ ,  $n_1$ ,  $n_2$ ,  $u_{ref}$ ,  $\Delta t$ ,  $\varphi_{ref}$ ,  $\vec{a} = [a_1 \ a_2]^T$ ,  $\vec{b} = [b_1 \ b_2 \ b_3]^T$ ,  $M$  are the structural parameters of the algorithm and are estimated empirically before the algorithm is applied.

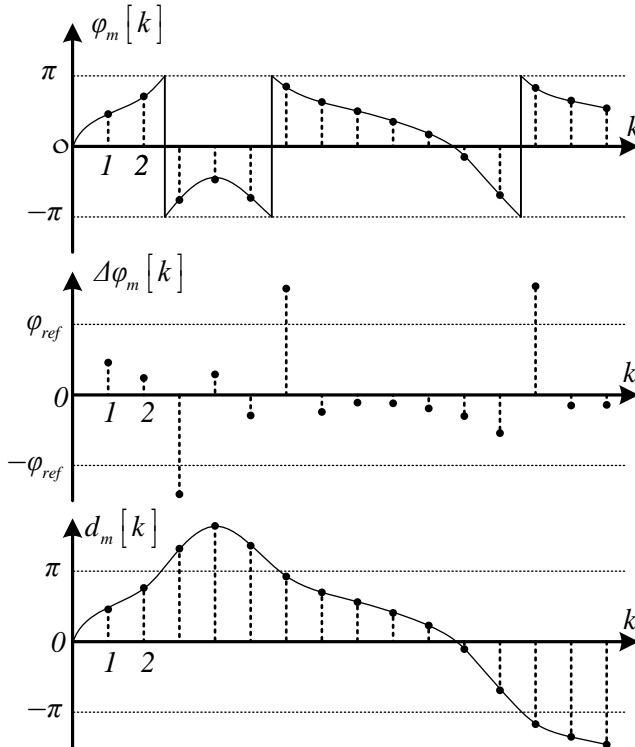


**Figure 2.** Applying the phase ambiguity resolution to improve the dynamic range of the displacement estimation.

Algorithm: displacement estimation

```

1 input:  $u$ 
2 output:  $\vec{d}=(d_1[k] \ d_2[k] \ \dots \ d_M[k])^T$ 
3 begin
4   multiply modulated signal by the carrier signal  $x_i=u_i \cdot v_i$ 
5   perform low pass filtering  $y_i=\vec{b}^T \vec{x}_i - \vec{a}^T \vec{y}_i$ 
6   if the  $k^{\text{th}}$  frame is ready then
7     if the  $k^{\text{th}}$  frame is the reference frame then
8       set the initial conditions
9        $\lambda_1[0] = \lambda_2[0] = \dots \lambda_M[0] = 0$ 
10       $\varphi_1[0] = \varphi_2[0] = \dots = \varphi_M[0] = 0$ 
11       $k=1$ 
12     else
13        $j$  – index of the reading corresponding to the moment  $t_2$  in the current frame,
14        $L$  – number of the readings in the interval  $\Delta t=[t_2 \dots t_3]$ 
15       extract the echo signal  $\vec{z}=(y_j \ y_{j+1} \ \dots \ y_{j+L})^T$ 
16        $\vec{\varphi}[k] = \arg(FFT[\vec{z}])$ 
17       for the  $m=1,2,\dots,M$  phase spectrum components do
18          $d_m[k] = \varphi_m[k] + \lambda_m[k] \cdot \pi$ 
19          $\Delta\varphi_m[k] = \varphi_m[k] - \varphi_m[k-1]$ 
20          $\lambda_m[k] = \lambda_m[k-1] + g(\Delta\varphi_m[k])$ 
21       end
22     end
23   end
24 end

```

#### 4. Results

The proposed method was used to process data gathered from the ultrasonic rangefinder in three experiments. For the first experiment a rectangular aluminum sheet was used as the object of interest (figure 3). A step motor with the step of the  $1.56 \mu\text{m}$  was used to cause the periodic sawtooth-like motion of the sheet with the amplitude of  $50 \mu\text{m}$  along the axis of the rangefinder's beam pattern.

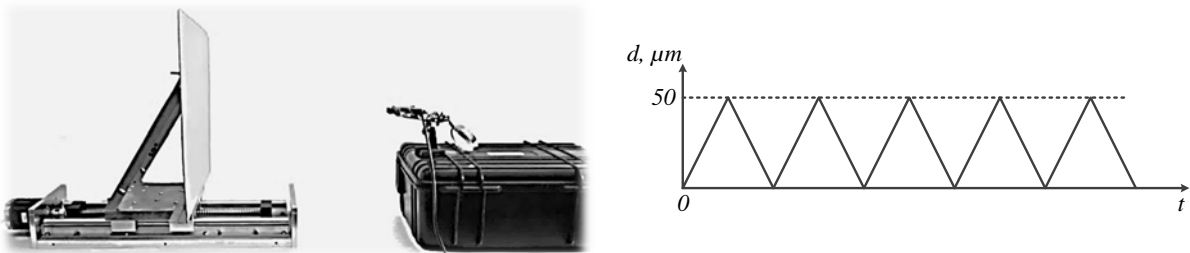


**Figure 3.** The experimental set-up and the sawtooth-like displacements of the sheet.

The 10 estimates of the aluminum sheet displacement with the amplitude of  $50 \mu\text{m}$  are shown in figure 4a. The figures 4b, 4c show the displacement estimates for the movements with the amplitude of  $4 \text{ mm}$  made by the proposed and the ToF methods respectively.

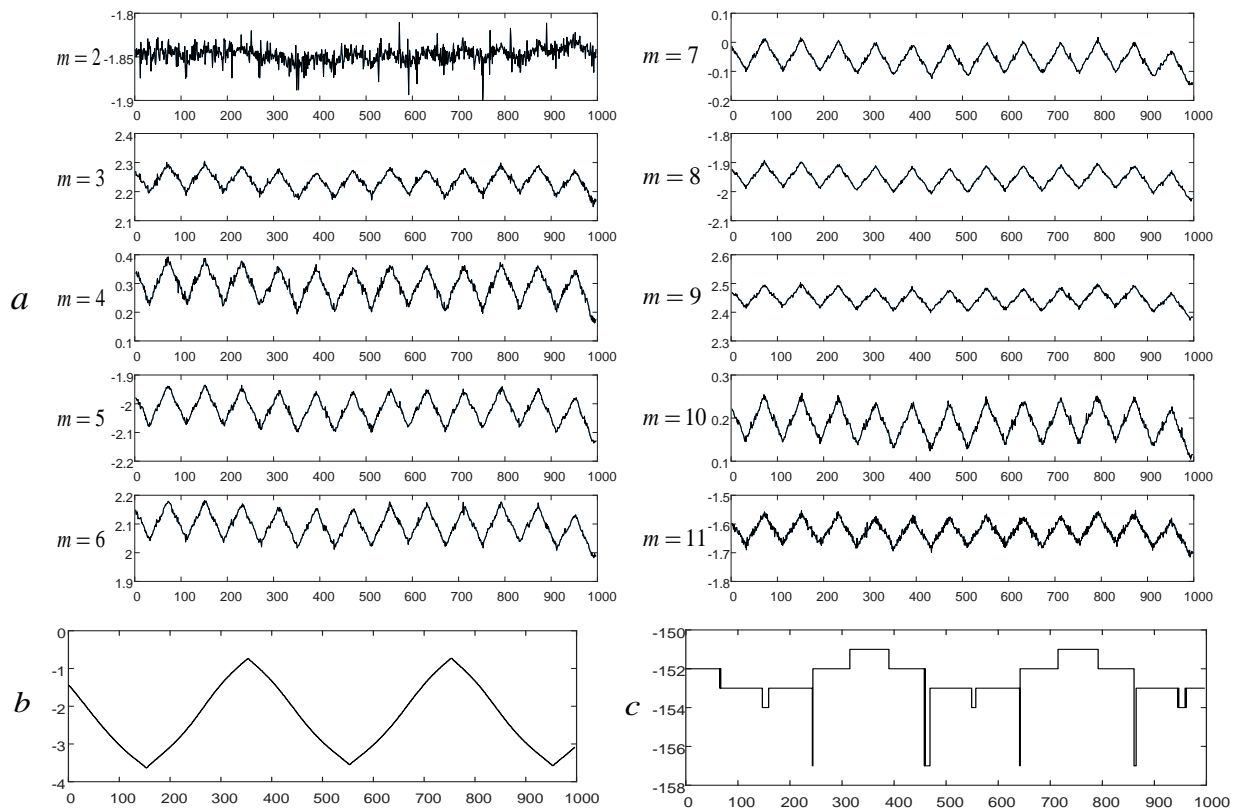


**Figure 4.** Aluminum sheet displacement estimates : a – 50  $\mu\text{m}$  amplitude, proposed algorithm, b – 4 mm amplitude, proposed algorithm, c – 4 mm amplitude, ToF method.

For the 2<sup>nd</sup> and the 3<sup>rd</sup> experiments the human chest was used as the object of interest. Figure 5 shows the 10 estimates of the human chest displacement during the respiration process computed using the proposed method.

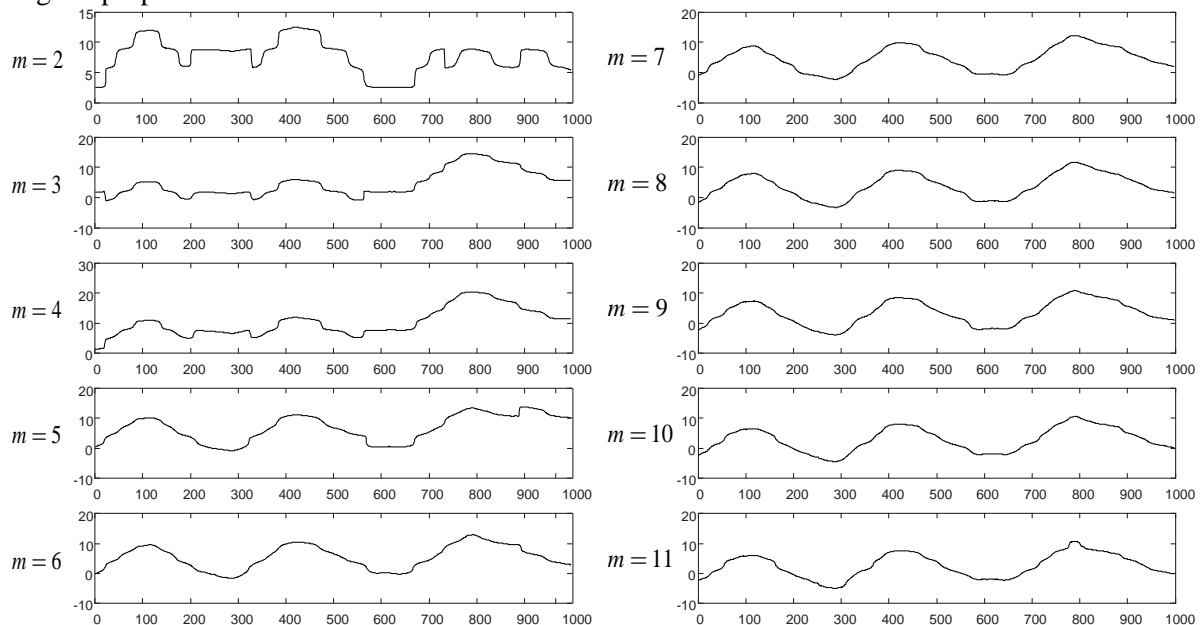


**Figure 5.** Human chest displacement during the respiration process.

Figure 6 contains the 10 estimates of the chest displacement caused by the cardiac activity while the person was holding their breath.

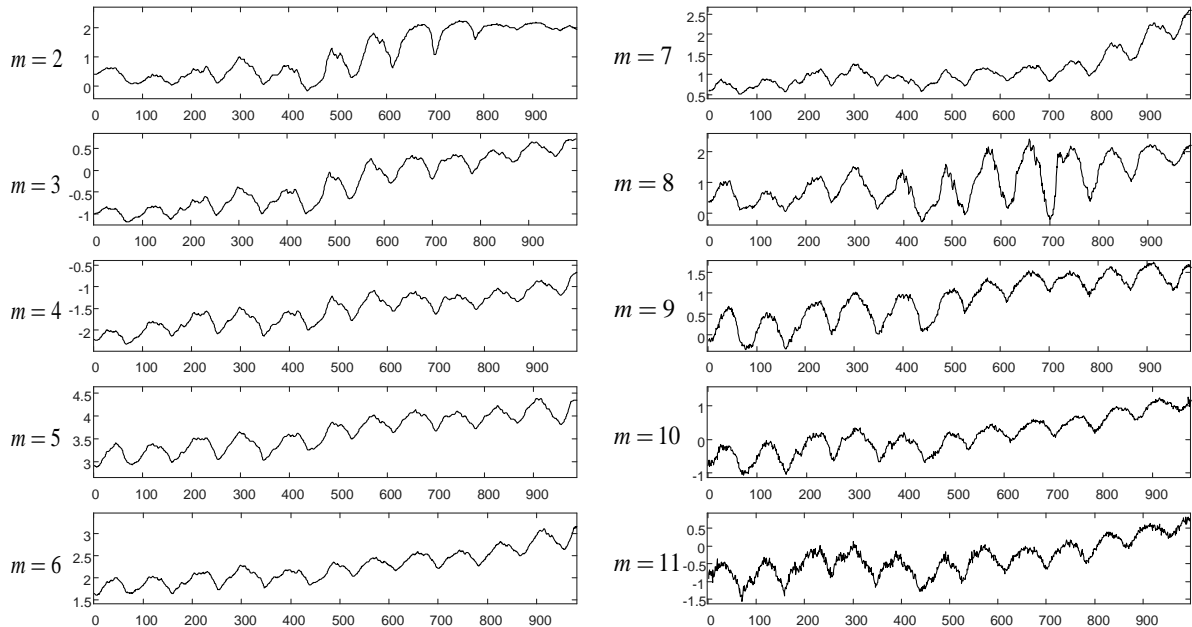


**Figure 6.** Human chest displacement caused by cardiac activity.

## 5. Conclusion

It is possible to empirically select the relevant (i.e., the most correlated with the object's movements) displacement estimates from the series computed by the proposed method. For the 1<sup>st</sup> experiment these estimates are under numbers 5, 6, 10, for the 2<sup>nd</sup> experiment these are estimates under numbers 7, 8, 9 and for the 3<sup>rd</sup> experiment these are estimates under numbers 5, 6, 8.

Since the aluminum sheet used in the 1<sup>st</sup> experiment was moving with the amplitude of the  $50 \mu\text{m}$ , we can make a rough estimate of the proposed method's resolution which is less than  $50 \mu\text{m}$  and, consequently, less than one hundredth of the ultrasonic wavelength with the frequency of  $f_{us} = 40 \text{ kHz}$  making it sufficient for the purposes of respiration and heartbeat detection. However, the aforementioned estimate is highly conservative and is a subject of the future research.

According to the experimental results, the ToF method is inadequate for the respiration and heartbeat graphs plotting due to its the measurement resolution. It should be also noted that in all of the experiments a considerable part of the target object was covered by the sensor's beam pattern and the waveform of the echo signal's envelope depends highly upon object's shape. So, in the 1<sup>st</sup> experiment all the surface points move equally linear, but in the 2<sup>nd</sup> and 3<sup>rd</sup> experiments the shape of the surface is a subject to the nonlinear three-dimensional changes causing sufficient changes in the waveform of the corresponding echo signal's envelope. For that reason the ToF-based results contain more noise for the 2<sup>nd</sup> and the 3<sup>rd</sup> experiments than for the 1<sup>st</sup>. Consequently, for the most of the applications the measurement resolution of this method is in close proximity to the wavelength.

Since the displacements caused by the respiration and heartbeat can be considered to be concentrated in the small neighborhood of  $d_{ref}$  it is possible to provide the accurate estimates based on the phase components. The proposed method is robust to such kind of the displacements since the only thing that changes during the process is the set of the relevant phase spectrum components. The main source of such robustness is the fact that both the time when the envelope exceeds the comparison threshold  $u_{ref}$  and all the information it contains are used to perform calculations.

However, to survive the significant nonlinear changes in the object's surface over time some combinations of the specific phase components should be used.

Therefore, the proposed method is suitable for the small movement detection happening in any region of the sensor's beam pattern and can be applied by mobile robots to detect human's vitals during the SAR operation.

An algorithm for the automatic selection of the most relevant phase spectrum components or combinations of these components based on the a-priori information about the target object and the measuring conditions poses another subject for a future research. Topics of interest also include the impact of the rough estimate  $d_{ref}$  on the relevant phase components selection and the compensation of the distortions caused by the air streams on the territory covered by the sensor's beam pattern.

- [1] Grigoryev E M, Gurzhin S G, Zhulev V I, Kaplan M B, Kryakov V G and Proshin E M 2016 Technology and methods for formation of the complex magnetotherapy impact by the inductor array, *5TH Mediterranean conference on embedded computing, MECO 2016*, Bar, Montenegro, June 2016, pp. 419-422.
- [2] Texas Instruments datasheet IWR1443 Single-Chip 76- to 81-GHz mmWave Sensor, SWRS211B –may 2017–revised February 2018.
- [3] Huang S S, Huang C F, Huang K N and Young M S 2002 A high accuracy ultrasonic distance measurement system using binary frequency shift-keyed signal and phase detection, *The Review of scientific instruments*, vol. 73, no. 10, pp. 3671-3677.
- [4] Saad A, Radwan A, Sadek S, Obeid S, Zaharia G and El Zein G 2009 Remote monitoring of heart and respiration rate using a wireless microwave sensor, *12th International Healthcare, Hospital Supplies and Medical Equipment Shows (Saudi Medicare 2009)*, Riad, Saudi Arabia, May 2009.
- [5] Huang Y P, Wang J S, Huang K N, Ho C T, Huang J D and Young M S 2007 Envelope pulsed ultrasonic distance measurement system based upon amplitude modulation and phase modulation, *The Review of scientific instruments*, vol.78, no. 6, 06510.